ACS APPLIED MATERIALS & INTERFACES

Research Article

www.acsami.org

Impact of Bimetal Electrodes on Dielectric Properties of TiO_2 and Al-Doped TiO_2 Films

Seong Keun Kim,† Sora Han, Woojin Jeon, Jung Ho Yoon, Jeong Hwan Han, Woongkyu Lee, and Cheol Seong Hwang*

WCU Hybrid Materials Program, Department of Materials Science and Engineering and Inter-university Semiconductor Research Center, Seoul National University, Seoul 151-744, Korea

ABSTRACT: Rutile structured Al-doped TiO_2 (ATO) and TiO_2 films were grown on bimetal electrodes (thin Ru/thick TiN, Pt, and Ir) for high-performance capacitors. The work function of the top Ru layer decreased on TiN and increased on Pt and Ir when it was thinner than ~2 nm, suggesting that the lower metal within the electrodes influences the work function of the very thin Ru layer. The use of the lower electrode with a high work function for bottom electrode eventually improves the leakage current properties of the capacitor at a very thin Ru top layer (≤2 nm) because of the increased Schottky barrier height at the interface between the dielectric and the bottom electrode. The thin Ru layer was necessary to achieve the rutile structured ATO and TiO_2 dielectric films.

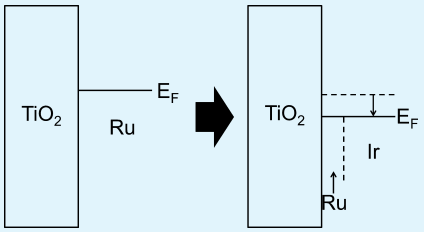

KEYWORDS: *TiO_2, bimetal layer electrode, work function*

INTRODUCTION

Rutile structured TiO_2 film has attracted a great deal of interest as a promising dielectric material for sub-30 nm technology dynamic random access memory capacitors due to its high dielectric constant (~100).[1] Although the small band gap (~3.1 eV) and n-type nature of the rutile structured TiO_2 raise high leakage currents, it was recently reported that doping Al ions into the rutile TiO_2 films remarkably improves the leakage properties because Al ions as an acceptor compensate for the n-type carrier in the rutile TiO_2 films, which eventually lower the Fermi level of the films.[2,3] As rutile-structured TiO_2 is a high-temperature phase, rutile-structured TiO_2 is seldom formed at typical atomic layer deposition (ALD) temperatures (<400 °C) and TiO_2 ALD generally forms anatase or amorphous TiO_2 with a relatively low dielectric constant. However, it was reported that in situ formed thin RuO_2 layer gives rise to the formation of rutile structured TiO_2 on Ru substrates by ALD with an oxygen source having a high oxidation potential such as O_3, O_2 or N_2O plasma because of the structural compatibility between rutile TiO_2 and the in situ formed RuO_2 layer at the interface.[1−8]

Although the use of the Ru substrate is an essential factor for the formation of rutile TiO_2, the low work function of Ru (~4.7 eV) results in higher leakage currents compared to the other noble metals like Pt (~5.6 eV) and Ir (~5.3 eV) having higher work functions. Han et al. recently demonstrated that the implementation of thick RuO_2 layer as the bottom electrode significantly improves the leakage properties of rutile structured TiO_2 based films (Al-doped TiO_2 (ATO) and TiO_2) compared to the use of the Ru electrode because of a higher work function (~5.0 eV) of the RuO_2 compared with Ru.[9] An interesting factor to note was that the in situ formed thin RuO_2/Ru has a lower work function than the thick RuO_2, suggesting that the lower Ru metal influences the work function of the RuO_2/Ru bilayer.

If the lower metal in a bimetal layer has an influence on the work function of the upper metal, the adoption of a metal with a higher work function as the lower metal in the bilayer can further improve the leakage properties of the dielectrics. In this study, therefore, electrically conducting materials such as TiN, Ir, and Pt, which have different work functions, were used as the lower electrode in the bimetal layer for the suppression of leakage currents for the given upper Ru metal layer. The Ru upper layer was indispensable in order to achieve the rutile phase TiO_2 during ALD. Ru films with various thicknesses were grown to the bottom metal layers by a pulsed chemical vapor deposition (p-CVD) or ALD method. The effect of Ru thickness on the crystalline phase and leakage properties regarding the TiO_2-based films grown on the top were studied in detail.

EXPERIMENTAL SECTION

TiO_2 and ATO films were grown at 250 °C by an ALD method using titanium tetrakis isopropoxide and trimethylaluminum as the Ti and Al sources, respectively. O_3 gas with a concentration of 380 g/m^3 was used as the oxygen source. Ti and Al precursor feeding and purge times were fixed at 2/0.5 and 5/5 s, respectively. O_3 feeding/purge time was fixed at 3/10 s. Sputtered 50-nm-thick TiN, Pt, and Ir films on SiO_2/Si substrates were used as the lower metal in the bimetal layer. Ru thin films with a thickness range of 1−8 nm were grown on these metal layers prior to the growth of TiO_2 and ATO films. The Ru films on the TiN substrates were grown by p-CVD with RuO_4 and N_2/H_2 as the reactants and the Ru films on the Pt and Ir substrates were

Received: June 19, 2012
Accepted: August 6, 2012
Published: August 6, 2012

   dx.doi.org/10.1021/am301094t | ACS Appl. Mater. Interfaces 2012, 4, 4726−4730

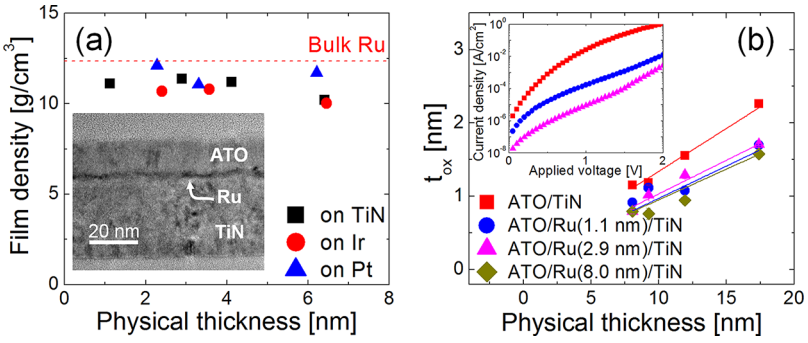

Figure 1. (a) Film density of Ru films grown on TiN, Pt, and Ir substrates evaluated by XRR. Inset: Cross-section TEM image of ATO film/1.1 nm thick Ru/TiN/SiO_2/Si. (b) Variation in the t_{ox} value as a function of the t_{phys} of ATO films grown on Ru/TiN and TiN electrodes. Inset figure: $J-V$ curves of 12 nm thick ATO films on TiN and 1.1 and 2.9 nm thick Ru/TiN, respectively.

grown by ALD with 2,4-(dimethylpentadienyl)(ethylcyclopentadienyl) Ru and O_2 as the reactants. The detailed deposition conditions for Ru layers were reported elsewhere.[10,11]

The crystalline structure of the TiO_2 films were analyzed by a glancing angle X-ray diffraction (GAXRD, PANalytical, X'pert Pro) at an incident beam angle of 1 °. Film thickness and density were evaluated by X-ray reflectivity (XRR) using the same equipment. The physical thickness and the continuity of the thin Ru films were confirmed by high-resolution transmission electron microscopy (HRTEM, JEOL, JEM 3000F). Furthermore, the work function of Ru films on the substrates was examined by Kelvin probe force microscopy (KPFM, JEOL, JSPM-5200).

Metal−insulator−metal capacitors were fabricated for the electrical measurement of the TiO_2 and ATO films. Top Pt electrodes were formed by a sputtering method using a shadow mask. All the capacitors were annealed at 400 °C under O_2 atmosphere after the fabrication of top Pt electrodes. The capacitance and leakage properties of the capacitors were measured using a Hewlett-Packard 4194A impedance analyzer and a 4140B pico-ammeter, respectively.

RESULTS AND DISCUSSION

First, the effects of thin Ru layers on TiN electrodes which have a low work function (~4.2 eV) are examined. Before the examination of the work function modulation, the formation of thin continuous and uniform Ru films on the TiN electrode should be verified. It is known that the nucleation of Ru by ALD and CVD processes is generally quite difficult on TiN surfaces resulting in island-like Ru films. The authors recently reported that a p-CVD process with RuO_4 and N_2/H_2 is capable of growing incubation-free Ru films on the TiN surface.[10] In this study, very thin Ru films with a thickness range of 1−8 nm formed on the TiN electrode by the p-CVD process. Figure 1a shows the film density of the Ru films on TiN, which is evaluated by XRR. The density of noncontinuous films such as island-like films should be much lower than the bulk value. The estimated Ru film density was approximately 11 g/cm^3, which is more than 90% of the bulk value (12.4 g/cm^3) and is maintained down to a film thickness of ~1 nm. This suggests that continuous Ru films were formed even at a thin thickness of ~1 nm. The slightly lower density of the Ru films compared with the bulk value is attributed to the characteristic of p-CVD Ru films rather than the formation of island-type films. The continuity of the 1.1 nm thick Ru film was also examined by cross-sectional HRTEM. Inset figure in Figure 1a shows a cross-sectional HRTEM image of an ATO/1.1 nm-thick Ru/TiN/SiO_2/Si stack. The thin Ru film is quite smooth and uniform on the TiN layer. The continuity of the Ru film was also confirmed in a wide area.

Electrical properties of ATO films on the various thickness Ru/TiN electrodes were examined. Figure 1b shows the variation in the equivalent oxide thickness (t_{ox}, which corresponds to the silicon oxide thickness to achieve the same capacitance density from the high-k material being used) value as a function of the physical thickness (t_{phy}) of ATO films grown on (RuO_2)/Ru/TiN and TiN electrodes. The dielectric constant of the ATO films, which is calculated from the inverse slope of the best-linear fitted graph ($\varepsilon_r = 3.9t_{phy}/t_{ox}$), is 33 on the TiN electrodes and 45−50 on 1.1−8.0 nm thick Ru/TiN electrodes, respectively. Here, the Al-concentration in the ATO film was ~12 at%. The difference in the dielectric constant of ATO films on the TiN and (RuO_2)/Ru/TiN electrodes is attributed to different crystalline structures. The authors reported that ALD TiO_2 films on TiN were crystallized into an anatase phase, while even the very thin Ru layer (~1.6 nm) on the TiN transformed the crystalline structure of the ALD TiO_2 films to a rutile phase with a high dielectric constant.[3] The high dielectric constant of the ATO films on the thin Ru/TiN electrode in this study is also due to the formation of the rutile phase. Inset figure in Figure 1b shows leakage current density versus applied voltage ($J-V$) curves of 12 nm thick ATO films on TiN and 1.1 nm- and 2.9 nm thick Ru/TiN, respectively. The ATO film on the TiN electrode showed very high leakage currents due to a low work function of TiN. Here, the top Pt electrode was positively biased, so that the $J-V$ curves represent the electron injection characteristics of the interface between the ATO and bottom electrodes. The ATO films on (RuO_2)/Ru/TiN exhibited better leakage properties than the ATO film on the TiN electrode. It is worth noting that the leakage properties of the ATO film on 2.9 nm-thick Ru/TiN is better than the properties of the ATO film on 1.1 nm thick Ru/TiN. The crystalline structure and the dielectric constant of the ATO films are identical on both (RuO_2)/Ru/TiN electrodes, suggesting that the difference in the leakage properties of the ATO films is not from the dielectric film itself. It was recently reported that a very thin conducting layer interposed between a thicker metal electrode and an insulator layer does not realize the bulk work function of the thin conducting layer.[12] It is likely that the deterioration in the leakage properties of the ATO film on thinner Ru/TiN results from lowering the work function of the Ru layer through the influence of the lower TiN electrode.

However, this also demonstrates that the use of a lower electrode with a higher work function can improve the leakage properties of rutile structured TiO_2 or ATO films, which was deposited on the thin Ru layer. Therefore, metal substrates such as Pt (work function ~5.6 eV) and Ir (work function ~5.3 eV)

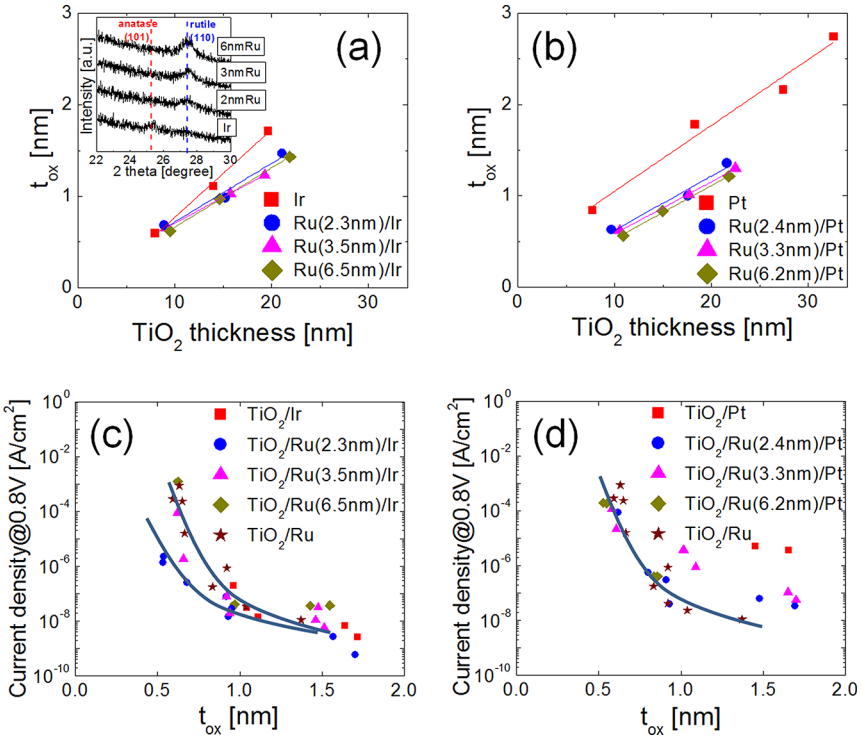

Figure 2. Variation in the t_{ox} value as a function of the t_{phy} for TiO_2 films on (a) thin Ru/Ir and (b) thin Ru/Pt electrodes, respectively. Inset in a: GAXRD patterns of ALD TiO_2 films on Ir and 2, 3, 6 nm thick Ru/Ir electrodes. *J* level at an applied voltage of 0.8 V vs t_{ox} value of the TiO_2 films on (c) Ru/Ir and (d) Ru/Pt electrodes,.

were attempted as the lower electrode for lower leakage currents. Very thin Ru films (2−7 nm) were grown on the Pt and Ir electrodes by ALD for the formation of rutile structured TiO_2 with a high dielectric constant. It was reported that continuous and smooth thin Ru films grow well on metallic surfaces by ALD due to the fluent nucleation of the Ru films on the top.[13,14] Ir also forms IrO_2, of which structure is also rutile forming the rutile phase TiO_2 on top, during the ALD of TiO_2 or ATO.[12] However, forming interfacial IrO_2 requires an extended O_3 pulse time, which is too long in order to make the ALD process practical. The Pt does not form any oxide, which is structurally compatible with the rutile TiO_2. Therefore, depositing the thin Ru is indispensable for these metal layers to form the rutile structured TiO_2 or ATO. As shown in Figure 1a, the relatively high film density of the ALD Ru films (10−11 g/cm^3) is maintained down to a thin thickness of ∼2 nm on Pt and Ir, which indicates the formation of continuous and smooth Ru films on these electrodes. Inset figure in Figure 2a shows GAXRD patterns of ALD TiO_2 films on Ir and 2, 3, 6 nm-thick Ru/Ir electrodes, respectively. The TiO_2 film on the Ir electrode shows a diffraction peak corresponding to an anatase phase, but the peak corresponding to the anatase completely disappeared for the TiO_2 films on all the Ru/Ir electrodes and those films are crystallized into a rutile phase.

Panels a and b in Figure 2 show variation in the t_{ox} value as a function of the t_{phy} regarding TiO_2 films on the thin Ru/Ir and the thin Ru/Pt electrodes, respectively. The dielectric constant of the TiO_2 films, which is calculated from the inverse slope of the linear fit graphs, is 40 and 33 on Pt and Ir electrodes, respectively, which is consistent with the anatase structure. However, the TiO_2 films on all the (RuO_2)/Ru/Pt or (RuO_2)/Ru/Ir electrodes have a higher dielectric constant of ∼70 due to the formation of the rutile phase. Panels c and d in Figure 2 exhibit the *J* level at an applied voltage of 0.8 V versus t_{ox} value of the TiO_2 films on (RuO_2)/Ru/Ir and (RuO_2)/Ru/Pt electrodes, respectively. For comparison, data of the TiO_2 films on (RuO_2)/Ru electrodes are also included in panels c and d in Figure 2. The TiO_2 films on (RuO_2)/Ru/Pt electrodes show similar dielectric performance irrespective of the thickness of the Ru layer. For the TiO_2 films on (RuO_2)/Ru/Ir electrodes, on the other hand, the TiO_2 films on 2.3 nm thick Ru/Ir demonstrate better leakage properties compared to the TiO_2 films on thicker Ru/Ir, which is in contrast to the case of ATO films on (RuO_2)/Ru/TiN electrodes where the thinner Ru layer showed a higher *J* level in Figure 1b.

To further elucidate the reason for this phenomenon, we examined the work function of the stack electrodes by KPFM. Figure 3a shows variation in the work function of Ru/Pt and Ru/Ir electrodes evaluated as a function of the Ru film thickness. The work function of the Pt and Ir electrodes was estimated to be 5.65 and 5.30 eV, respectively, which is consistent with the reported values, suggesting that the KPFM is reliable in order to estimate the work function of the metal

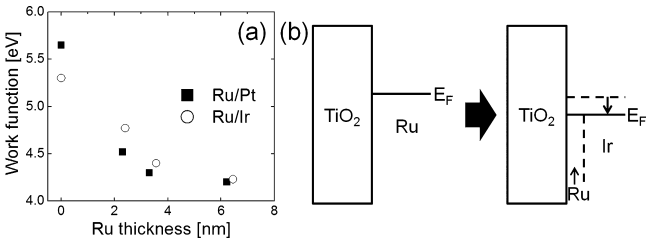

Figure 3. (a) Variation in the work function of the bimetal layers as a function of upper Ru thickness. (b) Schematic band diagram of TiO_2/metal before and after the insertion of an ultrathin Ru layer.

dx.doi.org/10.1021/am301094t | ACS Appl. Mater. Interfaces 2012, 4, 4726−4730

layers. The work functions decrease with increasing the thickness of the Ru layer and are saturated to ~4.2 eV above a Ru thickness of ~4−5 nm. An Ru layer approximately 2 nm-thick on the metal electrodes certainly has a higher work function than thicker Ru layers. This demonstrates that the improvement in the leakage properties of the TiO_2 films on 2 nm-thick Ru/Ir electrodes results from the increase of the Schottky barrier height due to the increase of the work function regarding the contact metal as schematically shown in Figure 3b. In spite of the higher work function of Pt, interestingly, the work function of Ru/Pt bilayers is lower than the value of Ru/Ir bilayers. The relatively low work function of Ru/Pt bilayers may lead to little difference in the leakage properties of the TiO_2 on Ru/Pt electrodes shown in Figure 2c. The low work function of Ru/Pt bilayers may be attributed to the differences in the Ru density or other unknown reasons, which are under investigation.

The opposite trend of leakage currents for the dielectric films on (RuO_2)/Ru/TiN bilayers with respect to the Ru thickness can be understood from the similar influence of thicker TiN layers on the work function of thin Ru layers. It should be noted that TiN has a lower work function than Ru while Ir has a higher work function than Ru. Therefore, this reveals that the lower electrode significantly influences the leakage properties of the capacitors at the very thin Ru layer (≤2 nm). As the Ru layer thickness increases, the work function of the Ru layer is recovered from the lowered value, so that the leakage current of the dielectric layer decreases. When two different metals come into contact with one another, electrons transfer from a metal with a low work function to a metal with a high work function in order to reach equilibrium. As the Ru layer becomes thinner than the critical thickness, in this work, ~2 nm, the free electron density in the Ru layer become decreased or increased due to their transport to or from the thicker bottom layers. Therefore, the very thin Ru layer loses its own work function and has a lower metal layer-dependent work function.

On the basis of the above discussion, the Ti-based capacitor system with excellent electrical performance was sought for. Figure 4 shows the *J*−*V* curves of ATO films grown on 2.3 nm-thick RuO_2/Pt and 2.3 nm thick RuO_2/Ir substrates. Herein, the Ru layer was replaced to RuO_2 since RuO_2 has a higher work function (~ 5.0 eV) than Ru. Although the thin Ru layer was supposed to be oxidized to RuO_2 or RuO_x during the ALD of TiO_2 or ATO, its quality was generally inferior to the deposited RuO_2, so that the deposition of the thin RuO_2 layer, instead of the oxidation of Ru, is beneficial in achieving a better property for the dielectric film.[9] The thin RuO_2 layer was also grown by the p-CVD with a shortened N_2/H_2 pulse time.[15] Both stacks show quite low leakage properties even at a quite low t_{ox} value of ~0.5 nm. However, the ATO/RuO_2/Ir stack with a t_{ox} of 0.5 nm showed an even lower leakage current (<1 × 10^{-8} A cm^{-2}) at an operation voltage of 0.8 V, compared with the other case, which is consistent with the results shown in Figure 3.

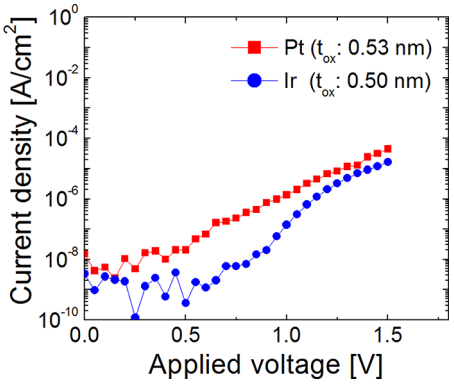

Figure 4. *J*−*V* curves of ATO films grown on 2.3 nm thick RuO_2/Pt and RuO_2/Ir.

CONCLUSIONS

In summary, rutile structured ATO and TiO_2 films were grown on bilayer electrodes such as Ru/TiN, Ru/Pt, and Ru/Ir. All the films showed high dielectric constants irrespective of the thickness regarding the Ru layer due to the formation of the rutile phase, resulting from the structural compatibility between rutile TiO_2 and in situ formed RuO_2 at the interface. The work function of a very thin Ru layer (≤2 nm) deposited on the lower metal in the bimetal layer was influenced by the work function of the thicker lower metal layer so were the leakage properties; the dielectric films on the thin Ru/TiN demonstrated inferior leakage properties than the films on the thick Ru/TiN while the TiO_2 films on the thin Ru/Ir exhibited better leakage properties than the films on the thick Ru/Ir. The lower and higher work function of TiN and Ir, respectively, compared with that of Ru, decreased and increased the work function of the thin Ru (or oxidized Ru) layer.

AUTHOR INFORMATION

Corresponding Author

*E-mail: cheolsh@snu.ac.kr.

Present Address

†Electronic Materials Research Center, Korea Institute of Science and Technology, Seoul, Korea, 130−650

Author Contributions

The manuscript was written through contributions of all authors. All authors have given approval to the final version of the manuscript.

Notes

The authors declare no competing financial interest.

ACKNOWLEDGMENTS

This study was supported by the IT R&D program of MKE/KEIT [KI002178, Development of a mass production compatible capacitor for next generation DRAM], Converging Research Center Program through the National Research Foundation of Korea (NRF) funded by the Ministry of Education, Science and Technology (2012K001299) and the Global Research Laboratory program (2012040157) through the NRF of Korea.

REFERENCES

(1) Kim, S. K.; Kim, W.-D.; Kim, K.-M.; Hwang, C. S.; Jeong, J. *Appl. Phys. Lett.* **2004**, *85*, 4112.
(2) Kim, S. K.; Choi, G.-J.; Lee, S. Y.; Seo, M.; Lee, S. W.; Han, J. H.; Ahn, H.-S.; Han, S.; Hwang, C. S. *Adv. Mater.* **2008**, *20*, 1429.
(3) Kim, S. K.; Lee, S. W.; Han, J. H.; Lee, B.; Han, S.; Hwang, C. S. *Adv. Func. Mater.* **2010**, *20*, 2989.
(4) Choi, G.-J.; Kim, S. K.; Won, S. J.; Kim, H. J.; Hwang, C. S. *J. Electrochem. Soc.* **2009**, *156*, G138.
(5) Kim, S. K.; Hwang, G. W.; Kim, W.-D.; Hwang, C. S. *Electrochem. Solid-State Lett.* **2006**, *9*, F5.

(6) Kim, S. K.; Lee, S. Y.; Seo, M.; Choi, G.-J.; Hwang, C. S. *J. Appl. Phys.* **2007**, *102*, 024109.
(7) Fröhlich, K.; Ťapajna, M.; Rosová, A.; Dobročka, E.; Hušeková, K.; Aarik, J.; Aidla, A. *Electrochem. Solid-State Lett.* **2008**, *11*, G19.
(8) Fröhlich, K.; Aarik, J.; Ťapajna, M.; Rosová, A.; Aidla, A.; Dobročka, E.; Hušková, K. *J. Vac. Sci. Technol. B* **2009**, *27*, 266.
(9) Han, J. H.; Han, S.; Lee, W.; Lee, S. W.; Kim, S. K.; Gatineau, J.; Dussarrat, C.; Hwang, C. S. *Appl. Phys. Lett.* **2011**, *99*, 022901.
(10) Han, J. H.; Lee, S. W.; Choi, G.-J.; Lee, S. Y.; Hwang, C. S.; Dussarrat, C.; Gatineau, J. *Chem. Mater.* **2009**, *21*, 207.
(11) Kim, S. K.; Lee, S. Y.; Lee, S. W.; Hwang, C. S.; Lee, J. W.; Jeong, J. *J. Electrochem. Soc.* **2007**, *154*, D95.
(12) Kim, S. K.; Han, S.; Han, J. H.; Lee, W.; Hwang, C. S. *Phys. Status Solidi RRL* **2011**, *5*, 262.
(13) Kim, S. K.; Han, J. H.; Kim, G. H.; Hwang, C. S. *Chem. Mater.* **2010**, *22*, 2850.
(14) Kim, S. K.; Han, S.; Kim, G. H.; Jang, J. H.; Han, J. H.; Hwang, C. S. *J. Electrochem. Soc.* **2011**, *158*, D477.
(15) Han, J. H.; Lee, S. W.; Kim, S. K.; Han, S.; Lee, W.; Hwang, C. S.; Dussarat, D.; Gatineau, J. *Chem. Mater.* **2012**, *24*, 1407.